Mice lacking NKCC1 are protected from development of bacteremia and hypothermic sepsis secondary to bacterial pneumonia

MyTrang Nguyen, Amy J. Pace, and Beverly H. Koller

Department of Genetics, University of North Carolina, Chapel Hill, NC 27599

The contribution of the Na^+-K^+-Cl^- transporter (NKCC1) to fluid in ion transport and fluid secretion in the lung and in other secretory epithelia has been well established. Far less is known concerning the role of this cotransporter in the physiological response of the pulmonary system during acute inflammation. Here we show that mice lacking this transporter are protected against hypothermic sepsis and bacteremia developing as a result of *Klebsiella pneumoniae* infection in the lung. In contrast, this protection was not observed in NKCC1$^{-/-}$ mice with *K. pneumoniae*—induced peritonitis. Although overall recruitment of cells to the lungs was not altered, the number of cells present in the airways was increased in the NKCC1$^{-/-}$ animals. Despite this robust inflammatory response, the increase in vascular permeability observed in this acute inflammatory model was attenuated in the NKCC1$^{-/-}$ animals. Our studies suggest that NKCC1 plays a unique and untoward unrecognized role in acute inflammatory responses in the lung and that specific inhibition of this NKCC isoform could be beneficial in treatment of sepsis.

CORRESPONDENCE
Beverly H. Koller:
treawouns@aol.com

Abbreviations: BAL, bronchoaveolar lavage; BALF, BAL fluid; CF, cystic fibrosis; MPO, myeloperoxidase; VCAM, vascular cell adhesion molecule.

Bacterial pneumonia remains a leading cause of death in humans, especially when complicated with bacteremia and sepsis. Conversely, sepsis resulting from primary infection at other sites is often complicated by the development of acute respiratory distress syndrome, and in fact, sepsis accounts for as many as half of all cases of acute respiratory distress syndrome (1–3). Lung injury often occurs at the onset of bacteremia, resulting in the failure of this organ. In both bacterial pneumonia and acute lung injury secondary to bacteremia, pathophysiological changes include compromise of the alveolar-capillary barrier which results in edema and consequently intravascular shunting and poor ventilation of the alveolus. Studies of sterile acute respiratory distress in dogs over 15 years ago suggested that the loop diuretic furosemide could decrease the intravascular shunt and improve pulmonary oxygen exchange (4). Clinical studies also suggested that this loop diuretic could improve pulmonary function of premature infants with chronic lung disease (5).

Loop diuretics such as furosemide and bumetanide block the activity of the two isoforms of the Na^+-K^+-$2Cl^-$ transporter, NKCC1 and NKCC2. Na^+-K^+-$2Cl^-$ cotransporters couple the electroneutral cellular uptake of one molecule of both Na^+ and K^+ with two molecules of Cl^- across the cell membrane. Under normal physiological conditions, NKCC cotransporters mediate a net influx of ions into cells because of the inwardly directed chemical gradients for Na^+ and Cl^- ions (6, 7). These systems are present in a broad spectrum of eukaryotic cells and are believed to play a central role in vectorial salt transport across epithelia and volume regulation in epithelial and nonepithelial cells (8, 9). Molecular studies have identified two isoforms, NKCC1 and NKCC2, that share ~60% identity (10–12). NKCC2 (*Slc12a1*) encodes a cotransporter expressed almost exclusively in the kidney, where it is found in the cells of the ascending loop of Henle (13–15). Here it plays a critical role in the vectorial transport of ions (Na^+, K^+, and Cl^-) from the glomerular ultra filtrate and hence is often referred to as the absorptive cotransporter. The fact that the improvement of the development of an intrapulmonary shunt after induction of acute lung injury was observed in dogs in which the kidneys had been surgically removed suggested that the beneficial effects of furosemide were not the result of blocking of this cotransporter (4). Similarly, in the premature infant, the improvement in gas exchange was more pronounced when furosemide was delivered as an aerosol, conditions under which the diuretic effects of this

The Journal of Experimental Medicine

agent were limited (5). Thus, both of these studies suggested that the beneficial effects of furosemide in models and patients with acute lung injury were the result of inhibition of the second transporter NKCC1.

The expression pattern of the *NKCC1* gene (*Slc12a2*) differs markedly from that of NKCC2 (16–18). NKCC1 is also expressed at high levels in the kidney, where in contrast to NKCC2, its expression is restricted to the medullary collecting duct and the glomerulus (15). Unlike NKCC2, the expression of NKCC1 is not limited to the kidney. NKCC1 is often referred to as the secretory cotransporter, because its expression is high in fluid-producing epithelia including the intestinal tract, salivary glands, submucosal glands, and the airway epithelia. However, pharmacological studies have identified furosemide-sensitive cotransporter activity in many cell types including hematopoietic cells, and airway and vascular smooth muscle. NKCC1 is believed to contribute to the regulation of cell volume in these nonepithelial cells (19). Of particular interest is the potential contribution of this transporter to the physiology of the endothelial cells, as they play a central role in many aspects of pneumonia and sepsis (20). Several studies suggest that NKCC1 regulates volume changes in these cells and that expression of NKCC1 by endothelial cells of the blood-brain barrier contributes to edema formation (21). It is therefore possible that similar expression of NKCC1 by lung endothelial cells can modulate the changes in microvascular permeability and thereby alter the course of inflammatory responses.

Mice lacking NKCC1 expression have been generated by several groups (22–26). The most readily observable phenotypes of the NKCC1$^{-/-}$ mice are their loss of hearing and inner ear function and male infertility. In addition, survival of the mice is limited on most genetic backgrounds, and generally those animals that do survive are considerably smaller in size. Most studies to date have been performed using mice of mixed genetic background. This has limited the use of these animals to study the role of NKCC1 during inflammatory responses, as the majority of these responses are sensitive to modifier genes (27, 28).

To circumvent this problem, in this study we generate congenic F1 NKCC1$^{-/-}$ mice and control littermates. We examine both the inflammatory response and the development

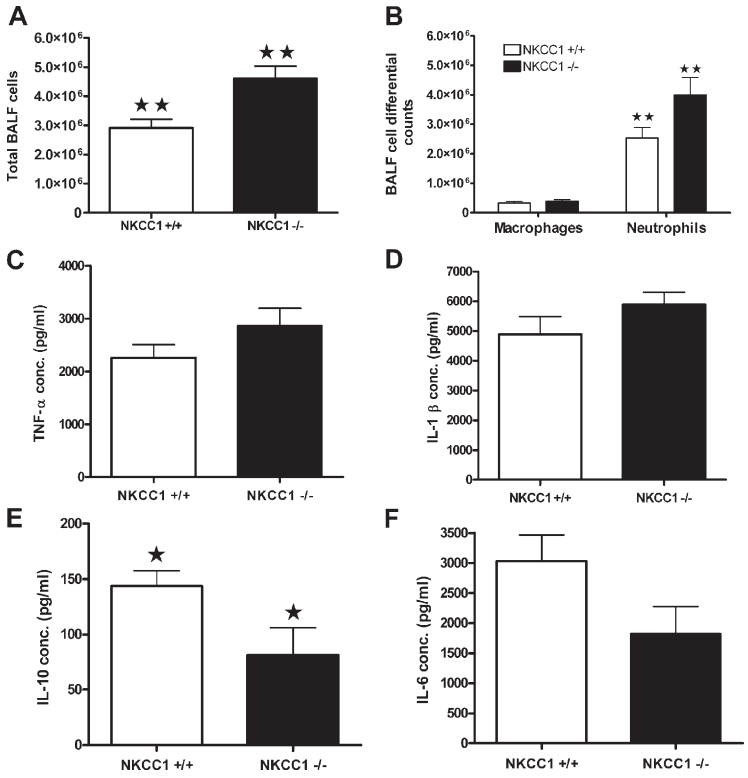

Figure 1. Inflammatory cells and cytokines present in BALF 48 h after infection with *K. pneumoniae*. (A) Total number of cells present in the airways and thus recovered by BAL was higher in the lungs of NKCC1$^{-/-}$ mice ($n = 30$) than NKCC1$^{+/+}$ mice ($n = 29$). (B) Cells present in the BAL were stained and identified based on morphological criteria. There was a statistically significant difference in the number of neutrophils in NKCC1$^{-/-}$ mice compared with wild-type controls. Macrophages remained unchanged in both groups. TNF-α, IL-1β, IL-10, and IL-6 levels were determined in the lung homogenates by ELISA kits. NKCC1$^{-/-}$ mice exhibited increased levels of (C) TNF-α and (D) IL-1β, but the increased levels did not reach statistical significance compared with littermate controls. (E) IL-10 levels were significantly reduced in NKCC1$^{-/-}$ mice compared with NKCC1$^{+/+}$ mice. (F) IL-6 levels were also reduced in NKCC1$^{-/-}$ mice in comparison to NKCC1$^{+/+}$ mice, but the reduced levels were not significant. Data are expressed as mean ± SEM; $n = 7$–10 mice per group for cytokine assays. *, $P < 0.05$; **, $P < 0.005$. conc., concentration.

of bacteremia and sepsis after lung infections with *Klebsiella pneumoniae* in these animals. We show that lack of the cotransporter reduces lung bacterial burden and dramatically reduces bacteremia and sepsis, which develops secondarily to this bacterial pneumonia.

RESULTS

Inflammation in NKCC1 mice after infection with *K. pneumoniae*

NKCC1$^{-/-}$ mice and littermate genetic controls were used to study the impact of loss of the cotransporter on the ability of the mice to mount a response to bacterial infection. In all cases, the mice were congenic F1 animals generated by the intercross of 129/SvEv$^{+/-}$ female animals with C57BL/6$^{+/-}$ males. Mice were infected with *K. pneumoniae*, and the development of disease was assessed 48 h later (Fig. 1). Mice were killed and the cells present in the airways were collected by bronchoalveolar lavage (BAL). As expected, the bacterial infection resulted in a dramatic increase in the number of cells present in the BAL fluid (BALF). However, the number of cells present in the BALF collected from NKCC1$^{-/-}$ animals was significantly higher ($P = 0.002$) than that collected from the normal littermates. Cells present in the BAL were stained and identified based on morphological criteria. As expected, the majority of the cells recovered were neutrophils, and this population was significantly increased ($P = 0.003$) in the NKCC1$^{-/-}$ mice.

We also examined the production of cytokines in the lung after infection with *K. pneumoniae*. Total lung homogenates were prepared from the lung 48 h after infection. As can be seen in Fig. 1, C–F, no differences were observed in the levels of TNF-α or IL-1β. However, a small but significant decrease ($P = 0.004$) in the level of IL-10 was observed in the NKCC1$^{-/-}$ mice. Overall, the levels of cytokines measured in the lungs of the NKCC1$^{-/-}$ and wild-type mice were remarkably similar given the difference in numbers of inflammatory cells in the airways.

To determine the impact of this difference in the number of neutrophils present in the airways on the progression of the infectious response in the mice, a second set of experiments was performed. Again the mice were infected with 4×10^4 bacteria. After 48 h mice were killed, blood was collected by heart stick, the lungs were collected and homogenized and CFUs in both samples were determined (Fig. 2). High levels of bacteria were detected in the blood of the wild-type mice. In contrast, loss of NKCC1 provided profound protection from the development of bacteremia with an almost 10-fold decrease in CFUs. This protection corresponded to decreased bacterial count in the homogenates prepared from the lungs of the NKCC1$^{-/-}$ animals compared with those prepared from wild-type mice. However, the difference in lung burden was not as dramatic as the difference observed upon comparison of CFUs present in the blood.

As expected, the high bacterial load and particularly the development of bacteremia corresponded with a marked hypothermia in the wild-type mice (Fig. 2 C). By 48 h, the profound drop in core temperature and the overall morbidity of the mice required that all animals in this group be killed. In comparison, the temperature of the NKCC1$^{-/-}$ mice remained well above 30°C, and the mice remained active throughout the time course of the experiment, consistent with the lower bacterial burden and the failure of the majority of these animals to develop substantial bacteremia.

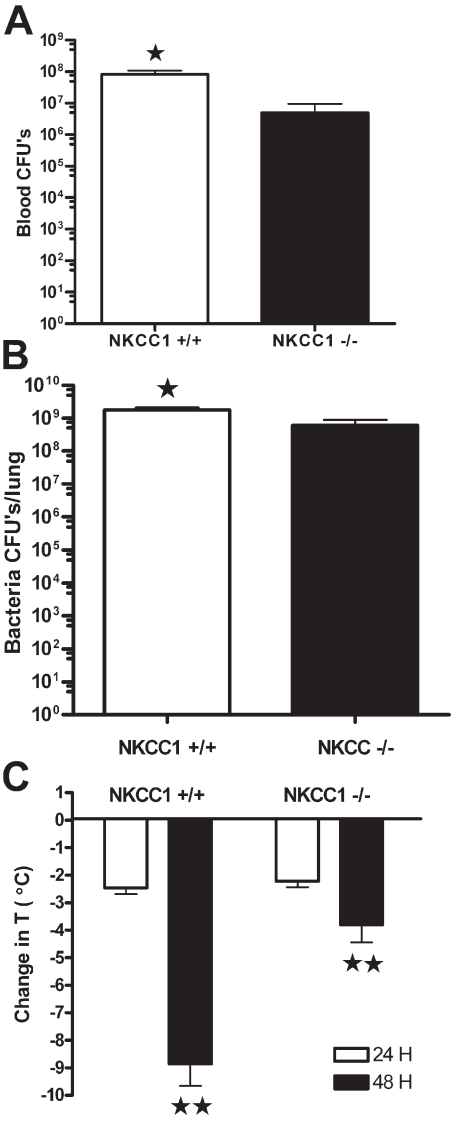

Figure 2. Colonization of the lung, bacteremia, and hypothermic sepsis after intertracheal infection of NKCC1$^{-/-}$ and control animals with *K. pneumoniae*. (A) Bacterial CFUs in the blood and (B) lung homogenates of NKCC1$^{-/-}$ mice ($n = 7$–8) were significantly lower than NKCC1$^{+/+}$ mice ($n = 10$–14). (C) Core temperatures of NKCC1$^{-/-}$ and wild-type littermates were determined before *K. pneumoniae* infection and 24 and 48 h thereafter. No differences were observed between the groups before inoculation or 24 h postinfection. However, the temperature drop observed in NKCC1$^{-/-}$ mice was significantly less than that measured for the NKCC1$^{+/+}$ mice 48 h postinfection. Values are shown as mean ± SEM; $n = 38$–43 mice per group. *, $P < 0.05$; **, $P < 0.000005$.

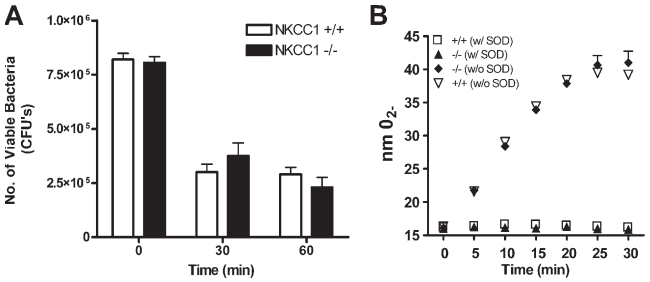

Figure 3. Oxidative burst and killing of *K. pneumoniae* by NKCC1$^{+/+}$ and NKCC1$^{-/-}$ neutrophils. (A) After 0, 30, and 60 min of incubation with *K. pneumoniae*, neutrophils isolated from the bone marrow of mice lacking NKCC1 did not differ from wild-type neutrophils in their ability to kill *K. pneumoniae* ex vivo. (B) Similarly, no difference was observed in superoxide production elicited by stimulation of the NKCC1$^{-/-}$ and NKCC1$^{+/+}$ neutrophils with PMA. Results are shown as mean ± SEM; $n = 5$ mice per group.

Bactericidal activity of NKCC1$^{-/-}$ and wild-type neutrophils

A role for ion transport in the development and function of the mature phagosome has been noted by others (29). We therefore reasoned that the difference in bacterial load and bacteremia could simply reflect differences in neutrophil function, specifically killing of *K. pneumoniae* by the phagocytes. To address this possibility, neutrophils were prepared from bone marrow of NKCC1$^{-/-}$ and control animals and cocultured with *K. pneumoniae*. To facilitate phagocytosis of the *K. pneumoniae*, the bacteria was treated with serum prepared from mice, which had been previously immunized with killed *K. pneumoniae*. As can be seen in Fig. 3 A, and as expected, the number of CFUs recovered from cultures containing neutrophils was significantly reduced compared with those cultures containing only bacteria, and this recovery decreased over the 1-h incubation period. However, no difference was observed between the ability of the NKCC1$^{-/-}$ and the wild-type neutrophils to eliminate the bacteria. Phagocytosis is normally accompanied by a dramatic increase in cellular oxygen metabolism. This "respiratory burst" results in the production of toxic reactive oxygen species essential for normal microbicidal activity of neutrophils. Neutrophils were isolated from the bone marrow of NKCC1$^{-/-}$ and control animals, and the production of superoxide in response to stimulation by PMA was determined. No difference was noted between the production of this reactive oxygen species by the two different populations of neutrophils (Fig. 3 B). These findings are consistent with the inability to detect measurable amounts of NKCC1 mRNA in the neutrophil by RT-PCR (Fig. 4).

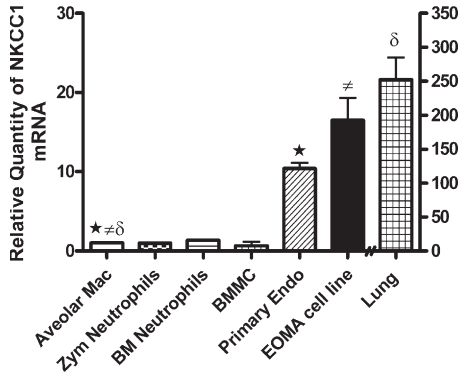

Figure 4. NKCC1 mRNA levels in lung and inflammatory cells. NKCC1 mRNA expression levels are significantly higher in the lung, an endothelial cell line (EOMA cell line, hemangioendothelioma origin, American Type Culture Collection no. CRL-2586), and primary lung endothelial cells (Primary Endo) relative to expression levels of zymosan-elicited neutrophils (Zym Neutrophils), bone marrow neutrophils (BM Neutrophils), BM mast cells (BMMC), and alveolar macrophages (Aveolar Mac). Data are expressed as mean ± SEM; $n = 5$ mice per group. *, ≠, δ, $P < 0.01$ relative to alveolar macrophage mRNA. Statistical analysis was performed using one-way ANOVA with Tukey's Multiple Comparisons posttest.

NKCC1$^{-/-}$ mice are not protected from *K. pneumoniae*–induced peritonitis

To determine if loss of NKCC1 generally attenuated bacterial growth and development of bacteremia and sepsis, we examined the consequence of *K. pneumoniae*–induced peritonitis in these animals and their littermate controls. Animals received an i.p. injection of 10^6 bacteria. To allow assessment of changes in vascular permeability resulting from challenge with this infectious agent, mice also received an i.v. injection of Evan's blue. This dye binds to serum proteins and thus provides a method of quantitation of extravasation of proteins from the circulatory system into the interstitial spaces and into the peritoneal cavity. 1 h later mice were killed, the peritoneal cavity was lavaged, and the number of CFUs present in the lavage fluid was determined. As can be seen in Fig. 5, in contrast to our findings in the lung, the bacterial burden of the NKCC1$^{-/-}$ mice did not differ significantly from that of the controls. Fewer leukocytes were present in the peritoneal cavity of the NKCC1$^{-/-}$ mice (Fig. 5 B). This did not, however, reflect a change in neutrophil recruitment but rather a change in the number of recovered macrophages (Fig. 5 C). Overall, the attenuated response noted in the NKCC1$^{-/-}$ mice in the bacterial pneumonia model was not apparent, at least at this time point, in the peritonitis model. Consistent with the decreased number of peritoneal leukocytes, the level of serum proteins present in the peritoneal lavage, as assessed by measuring Evan's blue levels, decreased in the NKCC1$^{-/-}$ animals (Fig. 5 D).

Sterile model of acute inflammation

We next determined whether similar differences between NKCC1$^{-/-}$ and wild-type mice in the influx of cells in response to inflammatory stimuli in the lung could be observed in a sterile model of inflammation (Fig. 6). NKCC1$^{-/-}$ and control mice received a single intratracheal bolus of LPS. 6 h later, the mice were killed, and the cells in the airways were collected and enumerated. As expected, LPS exposure resulted in a rapid increase in airway leukocytes, and this was

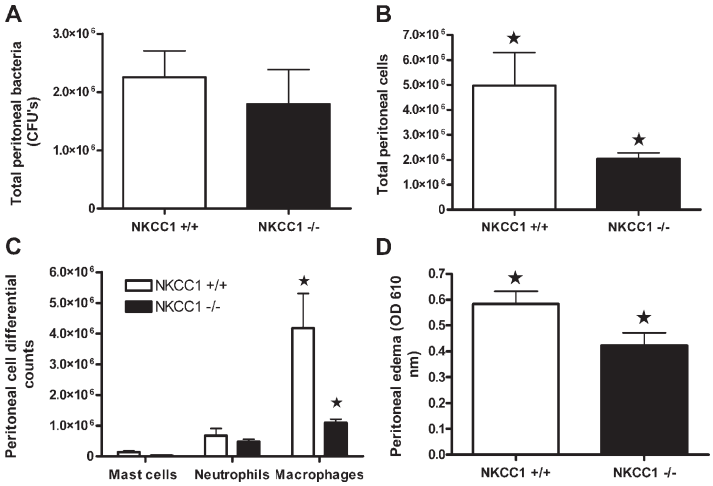

Figure 5. Assessment of bacterial load, cellular infiltrates, and edema formation after induction of peritonitis with *K. pneumoniae* in NKCC1$^{-/-}$ and wild-type mice. (A) CFUs in the peritoneal lavage fluid of NKCC1$^{+/+}$ and NKCC1$^{-/-}$ mice. Bacterial load was slightly lower in NKCC1$^{-/-}$ mice, but the reduced levels did not reach statistical significance (7–8 mice per group). (B) The total number of cells collected by peritoneal lavage was significantly decreased in NKCC1$^{-/-}$ mice compared with littermate controls ($P = 0.04$). (C) Differential cell counts were determined, based on morphological criteria, of cells present in the peritoneal lavage fluid of infected mice. A significant decrease was observed in the number of peritoneal macrophages in NKCC1-deficient mice compared with wild-type controls ($P = 0.016$). Emigrated neutrophils were present 1 h after *K. pneumoniae* infection. However, NKCC1-deficient mice showed no compromise in neutrophil emigration compared with NKCC$^{+/+}$ mice. (D) Consistent with a less robust inflammatory response, edema formation was significantly reduced in NKCC1$^{-/-}$ mice compared with littermate controls. Values are shown as mean ± SEM; $n = 15–18$ mice per group. *, $P < 0.05$.

largely attributable to the recruitment of neutrophils. Again the number of cells recovered from the NKCC1$^{-/-}$ airways was substantially greater than the number recovered from the wild-type mice. A significant increase in both the number of neutrophils ($P = 0.0001$) and the number of macrophages ($P = 0.004$) was observed in the mutant animals (Fig. 6 B). To determine whether the increased level of neutrophils in the airways and that collected by BAL reflected a general increase in sequestration of cells in the lung by animals lacking the cotransporter, we measured myeloperoxidase (MPO) levels in whole lung homogenates (Fig. 6 C). MPO is an enzyme primarily expressed by neutrophils and can be used as a surrogate marker for quantitation of tissue neutrophil levels. Surprisingly, although there was a trend toward higher levels, the total lung MPO levels did not differ much between the NKCC1$^{-/-}$ and the control animals. This suggests that although the overall number of neutrophils in the lungs was the same, the location of the neutrophils was altered in the absence of NKCC1, with cells moving into the airways and thus easily collected by lavage in the mutant animals. To further examine this point, an additional group of NKCC1$^{-/-}$ mice and littermate controls were treated with LPS. 12 h later the animals were killed and the lungs were inflated, fixed in paraformaldehyde, embedded in plastic, and thin sections were prepared. The number of inflammatory cells present in the airspaces in the two groups of animals was counted. Consistent with the increased neutrophil numbers in the BAL, a significantly higher number of neutrophils ($P = 0.02$) was observed in the alveolar spaces of the NKCC1$^{-/-}$ lungs compared with the control animals (Fig. 6, D and E). Similar to the studies of the *K. pneumoniae*–infected lungs, few differences were observed in the levels of cytokines present in the lungs of the wild-type and NKCC1$^{-/-}$ animals at this time point: no difference was observed in the levels of TNF-α, keratinocyte chemoattractant, or macrophage inflammatory protein 2, although a small difference was observed in IL-6 levels (Fig. 7).

To further delineate the mechanism by which loss of NKCC1 alters the acute inflammatory response of mice to LPS, we examined this response in bone marrow chimeras in which loss of cotransporter expression was confined to either the hematopoietic cells or to the parenchyma cells of the lung. Before initiating this line of experimentation, it was necessary to establish that lethal irradiation and reconstitution of mice with bone marrow did not itself alter the differential response of the NKCC1$^{-/-}$ and wild-type mice to LPS. As can be seen in Fig. 8, and as expected, an increase in total cell numbers in the BAL was observed in the NKCC1$^{-/-}$ animals that were irradiated and reconstituted with NKCC1$^{-/-}$ marrow compared with similarly treated wild-type animals. With this established, we generated bone marrow chimeras. NKCC1$^{-/-}$ mice were irradiated and reconstituted with wild-type marrow. Conversely, wild-type mice were reconstituted with bone marrow cells harvested from NKCC1$^{-/-}$ mice. These two groups were treated with LPS, and the recruitment of leukocytes to the lung was evaluated. The increase in influx of leukocytes into alveolar spaces correlated with the genotype of the recipient animals: an increase in the cellularity of the BAL was observed in the NKCC1$^{-/-}$ mice which received wild-type bone marrow cells. This strongly

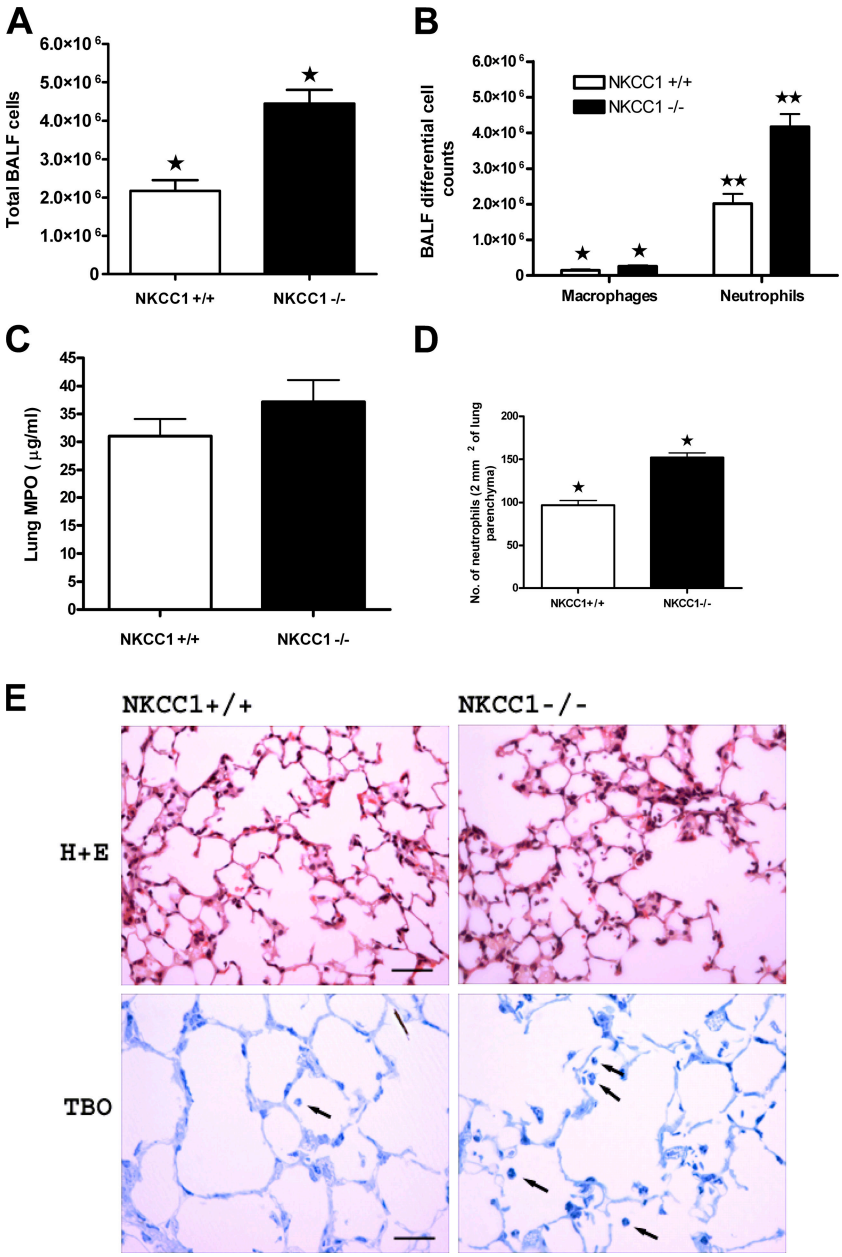

Figure 6. Examination of the response of NKCC1$^{-/-}$ and control animals in a sterile model of acute lung inflammation. The total number of cells in the BALF was enumerated (A), and populations of leukocytes were determined based on morphological criteria (B). The total number of cells in the BAL was significantly increased in LPS-challenged NKCC1$^{-/-}$ mice ($P = 0.00007$; $n = 11$) compared with the LPS-challenged NKCC1$^{+/+}$ mice ($n = 12$). Differential cell counts showed that this increase was the result primarily of increased numbers of neutrophils ($P = 0.0001$) although a small but significant increase in the number of macrophages was also observed ($P = 0.004$) in NKCC1-deficient mice compared with wild-type controls. To determine whether this difference represented a change in sequestration of neutrophils in the lung or specifically the movement of the cells into the airway, lungs were harvested from similarly treated animals, and the level of MPO in the lung was determined (C). MPO levels in the lungs of NKCC1$^{-/-}$ mice ($n = 11$) were higher than in the wild-type controls ($n = 12$), but the increased levels did not reach statistical significance. To directly visualize differences in the location of inflammatory cells in the two mouse lines, lungs were fixed and sections were prepared from LPS and saline-treated animals 12 h after exposure. Images similar to those shown in E were scanned and analyzed using Image Scope viewing software, and cells present in the airways were enumerated in a blinded fashion. The number of neutrophils present in the airways of the NKCC1$^{-/-}$ lungs ($n = 4$) was higher than in the control animals ($n = 4$) (D). All values are expressed as mean ± SEM. *, $P < 0.005$ and **, $P < 0.0005$. Bars: (top) 50 μm; (bottom) 100 μm.

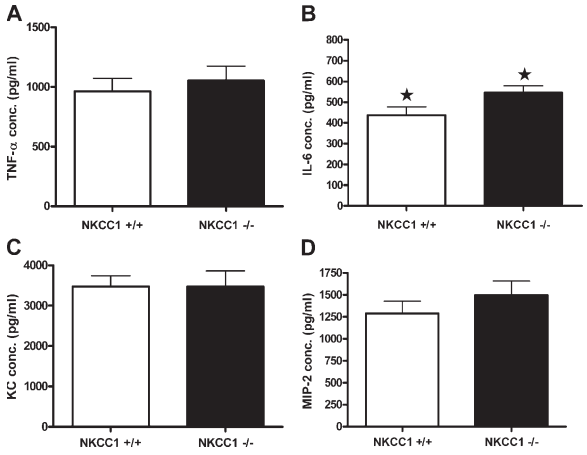

Figure 7. Inflammatory mediator levels in the lung homogenates of LPS-challenged NKCC1$^{+/+}$ and NKCC1$^{-/-}$ mice. No significant difference was observed in the levels of TNF-α, KC, and MIP-2 between NKCC1$^{+/+}$ and NKCC1$^{-/-}$ mice. However, NKCC1$^{-/-}$ mice ($P = 0.05$) exhibited slightly but significantly higher levels of IL-6 in comparison to littermate controls. Values are mean ± SEM from 11–12 mice per group. *, $P < 0.05$. conc., concentration.

indicates that loss of expression of NKCC1 on neutrophils is not responsible for the altered migration of the cells in response to LPS.

Attachment of neutrophils to activated endothelial cells is a prerequisite for recruitment during inflammatory responses. Activation of the endothelial cells results in expression of P and E selectins, which recognize L selectin expressed by neutrophils. Influx of neutrophils into the airways correlates with increased expression of vascular cell adhesion molecule (VCAM)-1. To determine whether the increased numbers of neutrophils could reflect altered induction of VCAM on endothelial cells, lungs were treated with LPS, and expression of VCAM was quantitated by Western blot analysis 6 h later (Fig. 9). As expected, LPS treatment results in an increase in levels of this protein. However, this change was observed in both NKCC1$^{-/-}$ and mutant mice and the magnitude of the change was similar in the two groups of animals.

Alterations in pulmonary vascular permeability in NKCC1$^{-/-}$ and wild-type mice after exposure to LPS

RNA expression analysis indicated that endothelial cells express NKCC1 (Fig. 4). Expression was easily detected both on a mouse endothelial cell line and on primary endothelial cell cultures, which we prepared from the mouse lung. Endothelial cells play a critical role both in sequestration of leukocytes and regulation of the permeability barrier of the pulmonary vasculature. Given the increased trafficking of cells into the airway and similarity in total numbers of neutrophils, we expected that the NKCC1$^{-/-}$ mice would display a similar or increased change in vascular permeability in the lung compared with their controls. To address this question, mice were treated with LPS to induce an inflammatory response (Fig. 10). Serum proteins were labeled by i.v. injection of animals with Evan's blue. At various times after exposure to LPS, mice were killed, the pulmonary vascular system was flushed with PBS, and the amount of dye present in the tissue was determined. In all cases the level of dye observed in control animals treated with vehicle was subtracted from the OD obtained from the LPS- treated animals. As expected, increased protein extravasation is observed 3 h after exposure to LPS. Surprisingly, the amount of serum protein present in the NKCC1$^{-/-}$ lungs was significantly decreased compared with that observed in wild-type animals (Fig. 10 A). Even at 6 h, when the edema is beginning to resolve, the difference between the two groups of animals persisted, suggesting that NKCC1 contributes to the changes in lung pulmonary vascular permeability during inflammation. To further address this point, we examined the lung wet to dry weight ratio of NKCC1$^{-/-}$ and control animals 3 h after instillation of LPS. This ratio was significantly reduced in the NKCC1$^{-/-}$ animals (Fig. 10 B).

DISCUSSION

Previous studies of the role of NKCC1 in the pathophysiology of infectious disorders have been limited for two reasons: (a) interpretation of traditional pharmacological studies using loop diuretics was difficult because these drugs inhibit both NKCC1 and NKCC2: inhibition of NKCC1 leads to dramatic changes in blood volume with broad physiological consequences; and (b) the use of mice lacking NKCC1 to address these questions has been complicated by the fact that survival and growth of these animals is compromised on inbred genetic backgrounds. We have circumvented these problems by generating a coisogenic and congenic 129/SvEv and C57BL/6 NKCC1-deficient mouse strain. Congenic F1 NKCC1$^{-/-}$ and control mice can then be generated by the intercross of these two lines. The survival of the 129B6F1 animals is greatly improved over that of C57BL/6 NKCC1$^{-/-}$ mice, and in addition, the size of the mice is within 10% of that of the wild-type controls. The availability of genetically identical control and experimental animals is essential in the experiments reported here, where large differences in the response of mice of various inbred backgrounds have been observed.

In our studies, we found that in the absence of NKCC1 expression colonization of the lungs with *K. pneumoniae* was reduced approximately threefold. Absence of the cotransporter had an even more dramatic effect on the development of bacteremia and sepsis. Although wild-type mice became moribund during the course of the experiment and were required to be killed within 48 h of intratracheal inoculation, the majority of the NKCC1$^{-/-}$ mice remained surprisingly healthy and active throughout the duration of the experiment. It is not clear at this point whether this dramatic difference in the development of hypothermic sepsis in the NKCC1$^{-/-}$ mice simply reflects the decreased bacterial burden in the lungs or whether other aspects of NKCC1 function also contribute to bacterial dissemination from the lung into the bloodstream.

It is unlikely that expression of NKCC1 on cells of hematopoietic origin contributes to the decreased morbidity of the

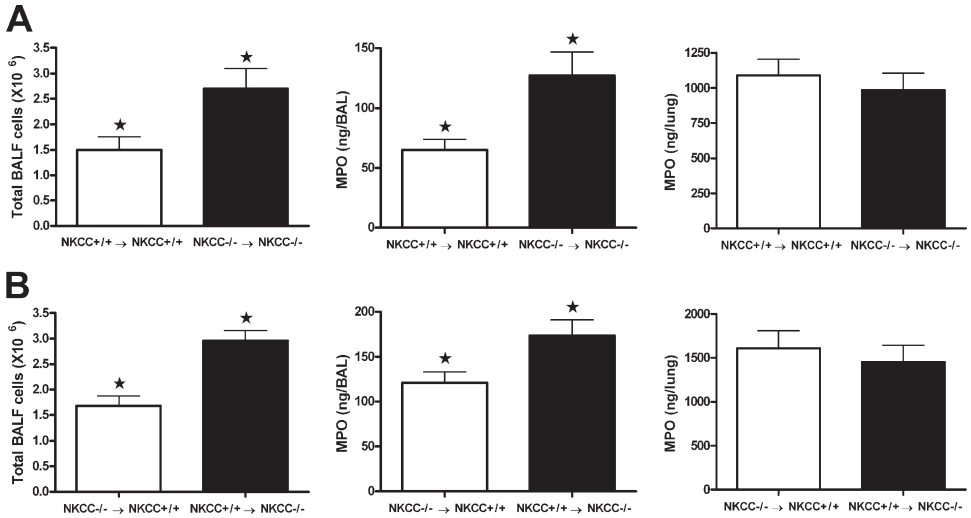

Figure 8. Evaluation of the contribution of NKCC1 expression by hematopoietic and lung cells to LPS-elicited neutrophil recruitment. We first performed an experiment to determine whether a difference in neutrophil recruitment and localization would continue to be observed in mice exposed to lethal doses of irradiation. NKCC1$^{-/-}$ and NKCC1$^{+/+}$ mice were lethally irradiated and reconstituted with genetically identical marrow (A). 6–8 wk after engraftment mice were challenged with LPS, the total cells in the BALF were enumerated, and the MPO content of the BAL and the lung was determined. As expected, we continued to observe an increase in the number of neutrophils present in the BAL, although no difference in the total number of cells recruited to the lung was apparent. To determine whether expression of NKCC1 by neutrophils contributes to the differential distribution of these cells, we generated a second cohort of mice. In this case, after irradiation, NKCC1$^{-/-}$ mice received marrow from wild-type animals (NKCC$^{+/+}\rightarrow$ NKCC$^{-/-}$), whereas NKCC1$^{+/+}$ mice received marrow from NKCC1$^{-/-}$ mice (NKCC$^{-/-}\rightarrow$ NKCC$^{+/+}$) (B). Higher cell counts in the BALF and higher MPO levels in the cells collected by lavage corresponded with loss of NKCC1 expression in the recipient, not the donor marrow (NKCC$^{+/+}\rightarrow$ NKCC$^{-/-}$, $n = 4$). Cell counts and MPO activity were significantly higher in these animals compared with wild-type animals in which the recipient expressed NKCC1 but was reconstituted with NKCC1$^{-/-}$ hematopoietic cells (NKCC$^{-/-}\rightarrow$ NKCC$^{+/+}$, $n = 6$). Again, no difference was observed between the groups in MPO activity in the lung. All values are expressed as mean ± SEM. *, $P < 0.05$.

NKCC1$^{-/-}$ mice. Levels of expression of NKCC1 detected by quantitative PCR are very low in neutrophils and macrophages. Consistent with this, no difference was observed in the ability of NKCC1-deficient neutrophils to kill *K. pneumoniae* in vitro or in the induction of a respiratory burst in response to PMA stimulation. Additionally, the study of bone marrow chimeras lacking NKCC1 on cells of hematopoietic lineages showed normal recruitment and localization of NKCC1$^{-/-}$ neutrophils when the lung expressed NKCC1. Increased numbers of neutrophils were collected by BAL from both *K. pneumoniae*–infected NKCC1$^{-/-}$ mice and NKCC1$^{-/-}$ mice treated with LPS. This indicates that the number of neutrophils that had both left the circulation and moved through the endothelial and epithelial tight junctions was increased in these animals. In contrast, little difference was seen in the number of neutrophils present in total lung homogenates from the LPS-challenged mice as determined by examination of myeloperoxidase levels. The most likely explanation for this is that change in expression of the co-transporter alters the pattern of neutrophil trafficking in the lung. It is possible that increased access to the airways results in enhanced clearance of *K. pneumoniae* and hence the decreased bacterial load.

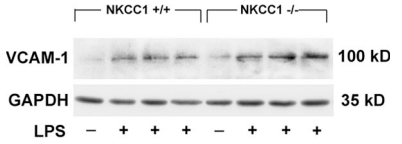

Figure 9. Western blot analysis of VCAM-1 after LPS stimulation. Lung lysates (100 μg of protein/lane) were subjected to Western blot analysis using polyclonal anti-mouse VCAM-1 antibody. GAPDH antibody was used as a loading control. Western blot analysis demonstrates an increase in VCAM-1 protein expression induced by LPS. However, the increased levels did not differ between NKCC1$^{+/+}$ and NKCC1$^{-/-}$ mice.

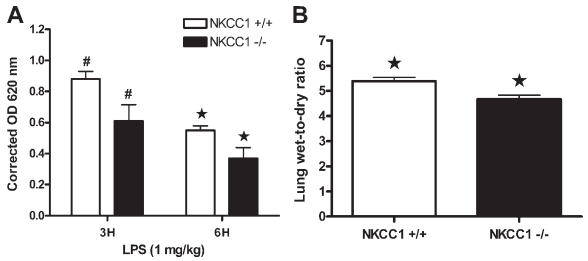

Figure 10. Changes in the permeability of lung capillaries after exposure of mice to LPS. Evan's blue extravasation was significantly lower in NKCC1$^{-/-}$ mice ($n = 7$) than in NKCC1$^{+/+}$ mice ($n = 6$) both 3 and 6 h after challenge. Similarly, a decrease in the wet-to-dry ratio was observed in the NKCC1$^{-/-}$ animals 3 h after LPS exposure ($n = 25$ NKCC1$^{+/+}$, $n = 18$ NKCC1$^{-/-}$). Data are expressed as mean ± SEM. *, #, $P < 0.05$.

NKCC1 is expressed by airway epithelial cells where it contributes to the formation of the airway surface liquid (30). NKCC1, located at the basolateral surface of the epithelium, works in tandem with cystic fibrosis transmembrane conductance regulator and Ca^{2+}-activated Cl^- channels to transport Cl^- across many secretory epithelia. In this regard it is intriguing that cystic fibrosis patients, who also have a disturbance in Cl^- secretion, have low incidence of sepsis despite high lung bacterial burdens. *Staphylococcus aureus* sepsis has not been described in CF patients, nor have invasive *Pseudomonas* infections been observed. One could speculate that the high levels of neutrophils in the CF lung also mimic what is observed in the NKCC1$^{-/-}$ mice. However, in the case of the CF patient, other factors and/or functions of CF render these recruited cells less effective at clearing the bacteria than appears to be the case in the NKCC1$^{-/-}$ mouse. For example, it has been suggested that CFTR directly regulates the activity of the epithelial sodium channel and thus that loss of CFTR results in Na^+ hyperabsorption and dehydration of the airway surface of CF patients. These alterations would counteract the beneficial effects of increased neutrophil recruitment into alveolar spaces in a manner that does not compromise barrier function. This could provide an explanation of why these patients, similar to the NKCC1$^{-/-}$ mice, appear protected from sepsis, but unlike the NKCC1$^{-/-}$ mice, have increased lung bacterial burdens.

The relatively high expression of NKCC1 on endothelial cells and the critical role of these cells in regulation of fluid flux into lung tissues raises the possibility that this may represent the key cell type responsible for the increased survival of the NKCC1$^{-/-}$ mice with pneumonia. Fluid flux into the alveolar spaces is regulated by the lung capillary barrier and compromise of the integrity of this barrier leads to edema and intrapulmonary shunting. Altered endothelial function is the principal reason for failure of the barrier (31). It is interesting to speculate that increases in permeability of the barrier require contraction of the endothelial cell and a change in cell shape, and that these events are accompanied by a change in cell volume. It is possible that NKCC1 is required for these changes and when cells lack the cotransporter these changes are compromised. If this is the case, our failure to observe a decrease in edema formation in *K. pneumoniae*–induced peritonitis would suggest that this function of NKCC1 is critical only in some capillary beds. An alternative model is suggested by studies which have demonstrated a role for NKCC1 in vascular tone (32). It is possible that decreased vascular pressure decreases edema formation in the lung. Again, in this model the contribution of NKCC1 to venous tone would be limited to specific vascular beds. The development of mouse lines in which loss of expression of NKCC1 is limited to specific tissues should help to distinguish between these various models.

In summary, we show here that loss of NKCC1 expression dramatically alters the course of bacterial pneumonia. Importantly, mice lacking the NKCC1 cotransporter were protected from sepsis and bacteremia. The impact of loss of NKCC1 was observed primarily in the lung. In contrast, the NKCC1$^{-/-}$ mice tended toward more severe disease when *K. pneumoniae* was introduced into the peritoneal cavity. Collectively, our results suggest that inhibitors specific for NKCC1 might provide a novel means of limiting sepsis in individuals with bacterial pneumonia. Given the profound impact of loss of NKCC1 on disease progression, it will be of great interest to more precisely define the mechanism underlying the attenuation of disease upon loss of NKCC1 activity. This should be possible with the development of culture conditions that allow in vitro study of endothelial barrier function of cells prepared from NKCC1$^{-/-}$ and control animals, and the generation of mouse lines in which the loss of expression of NKCC1 can be regulated in a cell type–specific manner.

MATERIALS AND METHODS

Animals. Mice were bred and maintained in pathogen-free animal facilities at the University of North Carolina at Chapel Hill in accordance with the Institutional Animal Care and Use Committee. The generation of NKCC1$^{-/-}$ mice has been described (25). F1 NKCC1-deficient and wild-type control mice were generated by crossing C57BL/6 congenic NKCC$^{+/-}$ mice (N12) to 129/SvEv$^{+/-}$ coisogenic mice.

Bacteria. Mouse virulent strain *K. pneumoniae* 43816, serotype 2, from the American Type Culture Collection were aerobically grown in nutrient broth for 2 h at 37°C. Bacteria numbers were estimated by measuring the absorbance at 600 nm (1 OD = 3×10^8 bacteria/ml) and exact number used in each experiment determining CFUs after plating an aliquot onto a nutrient agar plate.

***K. pneumoniae*–induced lung inflammation.** Mice were anesthetized, placed in an upright position, and suspended by the incisors over a supporting wire. The tongue was extended, and 4×10^4 CFU of *K. pneumoniae* in 50 μl PBS was delivered onto the vocal cords.

Assessment of lung inflammatory cells. 48 h postinfection with *K. pneumoniae* and 6 h after LPS challenge, the lungs were lavaged five times with Hanks' balance salt solution. The recovered BALF was pooled, and a 50-μl aliquot was reserved for determination of total cell counts with a hemacytometer. For differential cell counts, cytospin slides were prepared, stained using a Hema-3 staining kit (Fisher Scientific), and >200 leukocytes were identified based on morphological criteria per slide from each sample.

Assessment of *K. pneumoniae* in blood and lung tissues. 48 h postinfection with *K. pneumoniae*, mice were anesthetized and blood samples were obtained by cardiac puncture. Lungs were removed after pulmonary perfusion with PBS/5 mM EDTA and homogenized in a glass grinder with 2 ml of homogenate buffer (PBS with 1% Triton X-100) containing protease inhibitor tablet (Roche Diagnostics). Aliquots of the suspensions were plated onto LP plates, and CFUs were determined.

Cytokine and chemokine analysis postinflammation. After centrifugation of lung homogenates, supernatants were passed through a 0.45-μm syringe-driven filter unit to remove bacteria. TNF-α, IL-1β, IL-10, KC, and MIP-2 levels in supernatants and in BALF were determined by commercial ELISA kits (R&D Systems) according to the manufacturer's instructions.

Preparation of specific immune serum and opsonization of bacteria. Specific immune serum was prepared as described previously (33). Bacteria (10^7) were suspended in 1 ml of HBSS containing 1 mM $CaCl_2$, 0.5 mM $MgCl_2$ and 1 mM Hepes with 5% specific immune serum for 15 min at 37°C with end-to-end rotation before use.

Preparation of neutrophils and neutrophil-killing assays. Bone marrow was collected from mouse femurs and tibias, and neutrophils were isolated by density gradient centrifugation through 2 Histopaque layers (density 1.083 g/ml and 1.119 g/L; Sigma-Alrich). Preparations were > 90% pure as determined by staining with the Hema-3 staining kit (Fisher Scientific) and examination of cell morphology. Assessment of bacterial killing by neutrophils was performed as previously described (34, 35).

Measurement of superoxide production. Superoxide production was monitored by measurement of the superoxide dismutase–inhibitable cytochrome C reduction in a modification of methods described by Pick and Mizel (36). Superoxide produced by neutrophils was calculated from the extinction coefficient of cytochrome C by the formula $\Delta E_{550} = 210^3\ M^{-1}cm^{-1}$. The results were expressed as nanomoles of reduced cytochrome C.

LPS-induced lung inflammation. Anesthetized mice received 0.3 mg/kg of LPS (from *Escherichia coli*, Sigma-Aldrich) in 50 μl PBS intratracheally. 6 h later, mice were killed and harvested for assessment of airway inflammatory cells, mediator levels, and MPO activity.

MPO assay. MPO activity in lung tissues was measured 6 h after LPS exposure as described previously (37–41). MPO activity was quantified by extrapolation from the standard curve.

Lung permeability assay. Lung capillary permeability was determined by Evan's blue dye extravasation (42). 5 h after intratracheal challenge with LPS (1 mg/kg), mice received 10 mg/ml solution of Evan's blue dye i.v. (100 mg/kg). 1 h later, mice were killed and lungs were harvested after perfusion with HBSS and incubated in 2 ml of formamide at 55°C for 48 h. The absorbance of the Evan's blue extracts was spectrophotometrically measured at 620 and 740 nm. The following formula was used to correct for the presence of heme pigments: A_{620} (corrected) = $(1.426 \times A_{740} + 0.030)$.

Lung wet-to-dry weight ratio measurement. Mice were treated with LPS and 3 h later killed and whole lungs were excised and blotted dry and weighed. Lung dry weights were recorded after lung samples were dried in the oven for 3 d at 65°C. The lung wet-to-dry weight ratio was calculated by dividing the wet weight by the dry weight.

Isolation of pulmonary endothelial cells. Endothelial cells were isolated by magnetic cell sorting of labeled endothelial cells using a MACS separation unit (Miltenyi Biotec) as described previously by Marelli-Berg et al. (43). Endothelial cells were plated out onto 1% gelatin- (type B from bovine) coated tissue culture plates and cultured until confluent. At confluence, endothelial cells were characterized and RNA was prepared.

Quantitative RT-PCR. Total RNA was isolated using RNazol B (Teltest). Reverse transcription of RNA to cDNA for quantitative RT-PCR was performed using a high-capacity cDNA archive kit (Applied Biosystems) according to the manufacturer's instructions. Primers and probes were purchased from Applied Biosystems. All reactions were performed with TaqMan PCR Universal Master Mix (Applied Biosystems) using the Applied Biosystems 7900 HT Fast Real-Time PCR System. Reactions were performed in quadruplicate in a 20 μl final volume reaction. Expression levels of genes of interest were normalized to 18S RNA. Data were analyzed using the comparative C_T method as described by Applied Biosystems.

Lung histology. Mice received 0.3 mg/kg of LPS or vehicle intratraceally as described above. Mice were killed 12 h later and lungs were inflated, removed, and fixed in 2% paraformaldehyde/4% glutaraldehyde in Karlsson and Schultz sodium phosphate buffer at 4°C overnight. The left lobes were processed and embedded in paraffin wax. 4-μm-thick sections were cut and stained with hematoxylin and eosin. The other lobes were diced into small pieces and fixed again in glutaraldehyde fixative for 24 h. Subsequently, lung samples were postfixed in 1% osmium tetroxide, dehydrated in a graded ethanol series, and Epon infiltrated in an automated Reichert Lynx EM tissue processor. Specimens were embedded in Epon 812 and polymerized overnight at 65°C. 0.5-μm-thick sections were cut and stained with 1% Toluidine blue-O in 1% sodium borate. Slides were scanned with an Aperio ScanScope scanner (Aperio Technologies, Inc.) at 20× power to produce a high resolution digital image. Digital images were then analyzed using ImageScope viewing software (Aperio Technologies, Inc.), and neutrophils were counted in a blinded fashion.

***K. pneumoniae*–induced peritoneal inflammation.** Mice received 0.5% Evan's blue dye (Sigma-Aldrich) i.v. (10 mg/kg) followed by i.p injection of 10^6 CFU *K. pneumoniae*. 1 h after infection, mice were killed and the peritoneal cavities were lavaged with 4 ml of cold PBS. The number of peritoneal exudate cells in the peritoneal lavage fluid was determined by cell counts using a hemacytometer, and cellular differential were performed on cytospun slides. CFUs were determined after 18 h of incubation at room temperature on agar plates. Plasma protein extravasation into the peritoneal cavity was determined by measuring the absorbance of Evan's blue dye in the cell-free supernatants.

Western blotting. Lung lysates were prepared in lysis buffer. Samples (100 μg) were electrophoresed on 10% SDS-PAGE gels, and the proteins were electrophoretically transferred to PVDF membrane. Membranes were blocked in 5% nonfat milk in TBS with 0.1% Tween 20 for 1 h at room temperature and incubated overnight at 4°C with polyclonal anti–mouse VCAM-1 (R & D Systems, Inc.) at a final concentration of 0.1 μg/ml. Horseradish peroxidase–conjugated goat anti–mouse immunoglobulin G (Santa Cruz Biotechnology) was used as an appropriate secondary antibody. The blot was stripped and reprobed with anti-GAPDH (Imgenex) at a 1:5,000 dilution.

Generation of chimeric mice. Chimeric mice were generated using a previously described bone marrow transplantation method with modifications (44). In brief, whole bone marrow cells were harvested from femurs and tibias of 8-wk-old donor mice. Bone marrow cells were washed once, filtered through Miracloth (Calbiochem), and resuspended in PBS. Recipient mice were lethally irradiated with two exposures to 5 Gy 3 h apart. Immediately after the second exposure of irradiation, donor bone marrow cells were injected i.v into lethally irradiated recipient mice. Chimeric animals were used 6–8 wk after bone marrow transplantation.

Statistical analysis. Data are presented as mean ± SEM. Statistical comparisons between groups of mice were made by two-tailed Student's *t*-test. $P < 0.05$ was considered statistically significant.

This work was supported by National Institutes of Health grant R01 HL074583 (to B.H. Koller) and the Cystic Fibrosis Foundation grant Koller00Z0 (to B.H. Koller).

The authors would like to thank A. Latour for assistance with animal genotyping, B. Bagnell and V. Madden for assistance with microscopy, and L. Jania for statistical analysis.

The authors have no conflicting financial interests.

Submitted: 7 June 2006
Accepted: 24 April 2007

REFERENCES

1. Wheeler, A.P., and G.R. Bernard. 1999. Treating patients with severe sepsis. *N. Engl. J. Med.* 340:207–214.
2. Hudson, L.D., and K.P. Steinberg. 1999. Epidemiology of acute lung injury and ARDS. *Chest.* 116:74S–82S.
3. Hasleton, P.S., and T.E. Roberts. 1999. Adult respiratory distress syndrome—an update. *Histopathology.* 34:285–294.
4. Ali, J., W. Chernicki, and L.D. Wood. 1979. Effect of furosemide in canine low-pressure pulmonary edema. *J. Clin. Invest.* 64:1494–1504.
5. Prabhu, V.G., M. Keszler, and R. Dhanireddy. 1997. Pulmonary function changes after nebulised and intravenous frusemide in ventilated premature infants. *Arch. Dis. Child. Fetal Neonatal Ed.* 77:F32–F35.

6. Haas, M. 1994. The Na-K-Cl cotransporters. *Am. J. Physiol.* 267: C869–C885.
7. Russell, J.M. 2000. Sodium-potassium-chloride cotransport. *Physiol. Rev.* 80:211–276.
8. O'Grady, S.M., H.C. Palfrey, and M. Field. 1987. Characteristics and functions of Na-K-Cl cotransport in epithelial tissues. *Am. J. Physiol.* 253:C177–C192.
9. Haas, M., and B. Forbush III. 2000. The Na-K-Cl cotransporter of secretory epithelia. *Annu. Rev. Physiol.* 62:515–534.
10. Delpire, E., M.I. Rauchman, D.R. Beier, S.C. Hebert, and S.R. Gullans. 1994. Molecular cloning and chromosome localization of a putative basolateral Na(+)-K(+)-2Cl- cotransporter from mouse inner medullary collecting duct (mIMCD-3) cells. *J. Biol. Chem.* 269:25677–25683.
11. Payne, J.A., J.C. Xu, M. Haas, C.Y. Lytle, D. Ward, and B. Forbush III. 1995. Primary structure, functional expression, and chromosomal localization of the bumetanide-sensitive Na-K-Cl cotransporter in human colon. *J. Biol. Chem.* 270:17977–17985.
12. Park, J.H., and M.H. Saier. 1996. Phylogenetic, structural and functional characteristics of the Na-K-Cl cotransporter family. *J. Membr. Biol.* 149:161–168.
13. Gamba, G., A. Miyanoshita, M. Lombardi, J. Lytton, W.-S. Lee, M.A. Hediger, and S.C. Hebert. 1994. Molecular cloning, primary structure, and characterization of two members of the mammalian electroneutral sodium-(potassium)-chloride cotransporter family expressed in kidney. *J. Biol. Chem.* 269:17713–17722.
14. Igarashi, P., G.B.V. Heuvel, J.A. Payne, and B. Forbush III. 1995. Cloning, embryonic expression, and alternative splicing of a murine kidney-specific Na-K-Cl cotransporter. *Am. J. Physiol.* 269:f405–f418.
15. Payne, J.A., and B. Forbush III. 1994. Alternatively spliced isoforms of the putative renal Na-K-Cl cotransporter are differentially distributed within the rabbit kidney. *Proc. Natl. Acad. Sci. USA.* 91:4544–4548.
16. Lytle, C, J.-C. Xu, D. Biemesderfer, and B. Forbush III. 1995. Distribution and diversity of Na-K-Cl cotransport proteins: a study with monoclonal antibodies. *Am. J. Physiol.* 269:c1496–c1505.
17. Delpire, E., M.I. Rauchman, D.R. Beier, S.C. Hebert, and S.R. Gullans. 1994. Molecular cloning and chromosome localization of a putative basolateral Na^+-K^+-$2Cl^-$ cotransporter from mouse inner medullary collecting duct (mIMCD-3) cells. *J. Biol. Chem.* 269:25677–25683.
18. Xu, J.-C., C.Y. Lytle, T.T. Zhu, J.A. Payne, E. Benz Jr., and B. Forbush III. 1994. Molecular cloning and functional expression of the bumetanide-sensitive Na-K-Cl cotransporter. *Proc. Natl. Acad. Sci. USA.* 91:2201–2205.
19. O'Donnell, M.E. 1993. Role of Na-K-Cl cotransport in vascular endothelial cell volume regulation. *Am. J. Physiol.* 264:C1316–C1326.
20. Aird, W.C. 2003. The role of the endothelium in severe sepsis and multiple organ dysfunction syndrome. *Blood.* 101:3765–3777.
21. O'Donnell, M.E., L. Tran, T.I. Lam, X.B. Liu, and S.E. Anderson. 2004. Bumetanide inhibition of the blood-brain barrier Na-K-Cl cotransporter reduces edema formation in the rat middle cerebral artery occlusion model of stroke. *J. Cereb. Blood Flow Metab.* 24:1046–1056.
22. Dixon, M.J., J. Gazzard, S.S. Chaudhry, N. Sampson, B.A. Schulte, and K.P. Steel. 1999. Mutation of the Na-K-Cl co-transporter gene *Slc12a2* results in deafness in mice. *Hum. Mol. Genet.* 8:1579-1584.
23. Delpire, E., J. Lu, R. England, C. Dull, and T. Thorne. 1999. Deafness and imbalance associated with inactivation of the secretory Na-K-2Cl co-transporter. *Nat. Genet.* 22:192–195.
24. Flagella, M., L.L. Clarke, M.L. Miller, L.C. Erway, R.A. Giannella, A. Andringa, L.R. Gawenis, J. Kramer, J.J. Duffy, T. Doetschman, et al. 1999. Mice lacking the basolateral Na-K-2Cl cotransporter have impaired epithelial chloride secretion and are profoundly deaf. *J. Biol. Chem.* 274:26946–26955.
25. Pace, A.J., E. Lee, K. Athirakul, T.M. Coffman, D.A. O'Brien, and B.H. Koller. 2000. Failure of spermatogenesis in mouse lines deficient in the Na+-K+-2Cl- cotransporter. *J. Clin. Invest.* 105:441–450.
26. Pace, A.J., V.J. Madden, O.W. Henson Jr., B.H. Koller, and M.M. Henson. 2001. Ultrastructure of the inner ear of NKCC1-deficient mice. *Hear. Res.* 156:17–30.
27. Thach, D.C., T. Kimura, and D.E. Griffin. 2000. Differences between C57BL/6 and BALB/cBy mice in mortality and virus replication after intranasal infection with neuroadapted Sindbis virus. *J. Virol.* 74:6156–6161.
28. Weinberg, J.B., M.L. Lutzke, R. Alfinito, and R. Rochford. 2004. Mouse strain differences in the chemokine response to acute lung infection with a murine gammaherpesvirus. *Viral Immunol.* 17:69–77.
29. Segal, A.W. 2005. How neutrophils kill microbes. *Annu. Rev. Immunol.* 23:197–223.
30. Grubb, B.R., A.J. Pace, E. Lee, B.H. Koller, and R.C. Boucher. 2001. Alterations in airway ion transport in NKCC1-deficient mice. *Am. J. Physiol. Cell Physiol.* 281:C615–C623.
31. Dudek, S.M., and J.G. Garcia. 2001. Cytoskeletal regulation of pulmonary vascular permeability. *J. Appl. Physiol.* 91:1487–1500.
32. Meyer, J.W., M. Flagella, R.L. Sutliff, J.N. Lorenz, M.L. Nieman, C.S. Weber, R.J. Paul, and G.E. Shull. 2002. Decreased blood pressure and vascular smooth muscle tone in mice lacking basolateral Na(+)-K(+)-2Cl(-) cotransporter. *Am. J. Physiol. Heart Circ. Physiol.* 283: H1846–H1855.
33. Mancuso, P., T.J. Standiford, T. Marshall, and M. Peters-Golden. 1998. 5-Lipoxygenase reaction products modulate alveolar macrophage phagocytosis of Klebsiella pneumoniae. *Infect. Immun.* 66:5140–5146.
34. Rubin, B.B., G.P. Downey, A. Koh, N. Degousee, F. Ghomashchi, L. Nallan, E. Stefanski, D.W. Harkin, C. Sun, B.P. Smart, et al. 2005. Cytosolic phospholipase A2-alpha is necessary for platelet-activating factor biosynthesis, efficient neutrophil-mediated bacterial killing, and the innate immune response to pulmonary infection: cPLA2-alpha does not regulate neutrophil NADPH oxidase activity. *J. Biol. Chem.* 280:7519–7529.
35. Dziarski, R., K.A. Platt, E. Gelius, H. Steiner, and D. Gupta. 2003. Defect in neutrophil killing and increased susceptibility to infection with nonpathogenic gram-positive bacteria in peptidoglycan recognition protein-S (PGRP-S)-deficient mice. *Blood.* 102:689–697.
36. Pick, E., and D. Mizel. 1981. Rapid microassays for the measurement of superoxide and hydrogen peroxide production by macrophages in culture using an automatic enzyme immunoassay reader. *J. Immunol. Methods.* 46:211–226.
37. Mehrad, B., R.M. Strieter, T.A. Moore, W.C. Tsai, S.A. Lira, and T.J. Standiford. 1999. CXC chemokine receptor-2 ligands are necessary components of neutrophil-mediated host defense in invasive pulmonary aspergillosis. *J. Immunol.* 163:6086–6094.
38. Manderscheid, P.A., R.P. Bodkin, B.A. Davidson, E. Jensen, T.A. Russo, and P.R. Knight. 2004. Bacterial clearance and cytokine profiles in a murine model of postsurgical nosocomial pneumonia. *Clin. Diagn. Lab. Immunol.* 11:742–751.
39. Shao, C., J. Qu, L. He, Y. Zhang, J. Wang, Y. Wang, H. Zhou, and X. Liu. 2005. Transient overexpression of gamma interferon promotes Aspergillus clearance in invasive pulmonary aspergillosis. *Clin. Exp. Immunol.* 142:233–241.
40. Power, M.R., Y. Peng, E. Maydanski, J.S. Marshall, and T.J. Lin. 2004. The development of early host response to *Pseudomonas aeruginosa* lung infection is critically dependent on myeloid differentiation factor 88 in mice. *J. Biol. Chem.* 279:49315–49322.
41. Jain-Vora, S., A.M. LeVine, Z. Chroneos, G.F. Ross, W.M. Hull, and J.A. Whitsett. 1998. Interleukin-4 enhances pulmonary clearance of *Pseudomonas aeruginosa*. *Infect. Immun.* 66:4229–4236.
42. Wang, E., N. Ouellet, M. Simard, I. Fillion, Y. Bergeron, D. Beauchamp, and M.G. Bergeron. 2001. Pulmonary and systemic host response to *Streptococcus pneumoniae* and *Klebsiella pneumoniae* bacteremia in normal and immunosuppressed mice. *Infect. Immun.* 69:5294–5304.
43. Marelli-Berg, F.M., E. Peek, E.A. Lidington, H.J. Stauss, and R.I. Lechler. 2000. Isolation of endothelial cells from murine tissue. *J. Immunol. Methods.* 244:205–215.
44. Fabre, J.E., J.L. Goulet, E. Riche, M. Nguyen, K. Coggins, S. Offenbacher, and B.H. Koller. 2002. Transcellular biosynthesis contributes to the production of leukotrienes during inflammatory responses in vivo. *J. Clin. Invest.* 109:1373–1380.